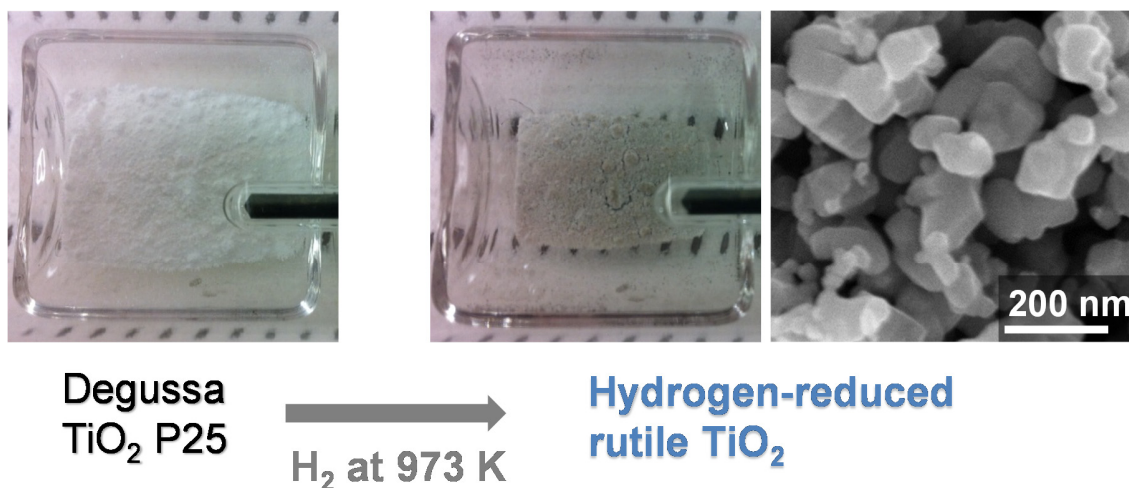


Supplementary Information for

**Rutile Titanium Dioxide Prepared by Hydrogen
Reduction of Degussa P25 for Highly Efficient
Photocatalytic Hydrogen Evolution**

Fumiaki Amano^{a}, Masashi Nakata^a, Akira Yamamoto^{b,c}, and Tsunehiro Tanaka^{b,c}*



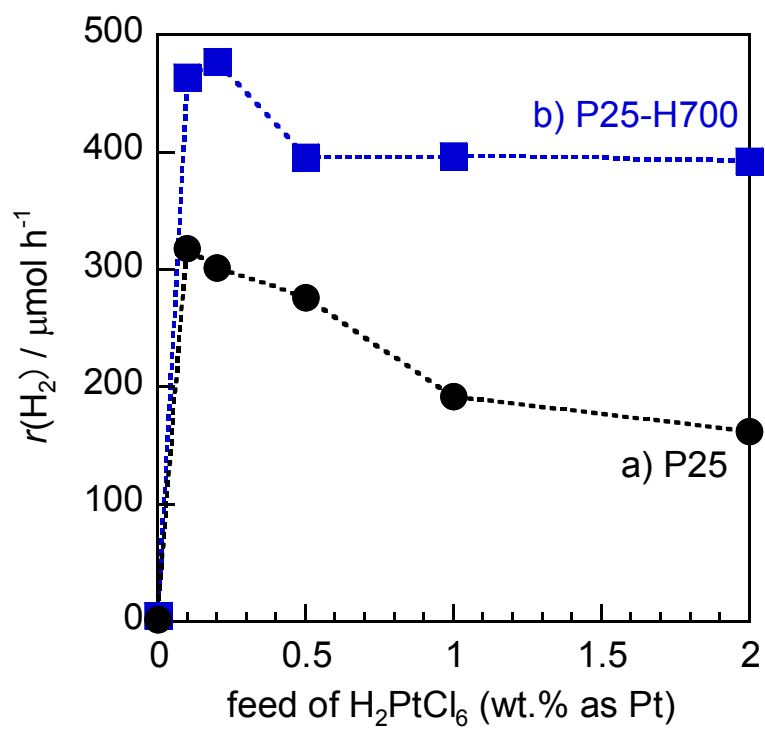


Figure S1. Effect of Pt loading (feed of $\text{H}_2[\text{PtCl}_6]$) on the rate of photocatalytic H_2 evolution from 50 vol.% aqueous ethanol solutions over (a) P25 and (b) P25-H700 with Pt under 380-nm irradiation.

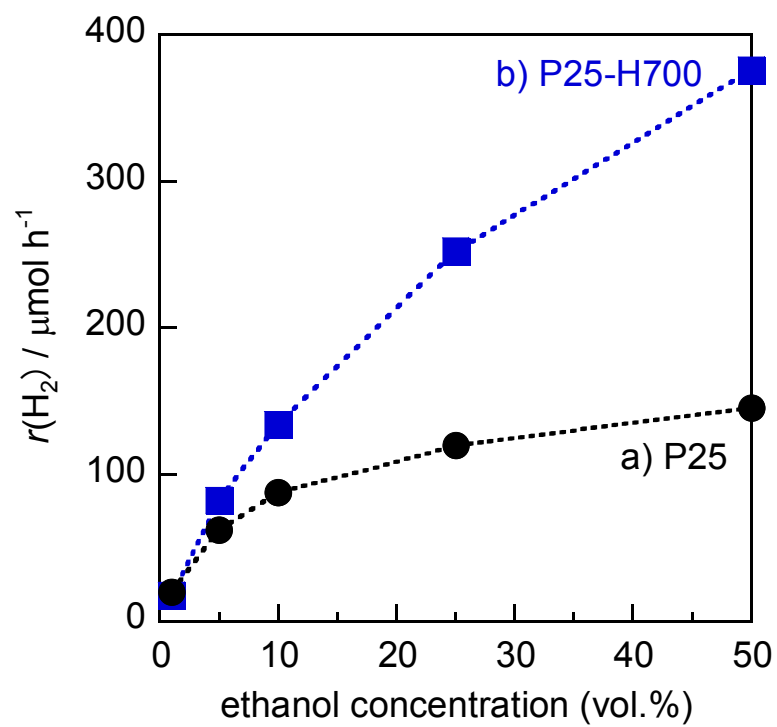


Figure S2. Effect of ethanol concentration on the rate of photocatalytic H₂ evolution from aqueous ethanol solutions over (a) P25 and (b) P25-H700 with 2.0 wt.% Pt under 380-nm irradiation.

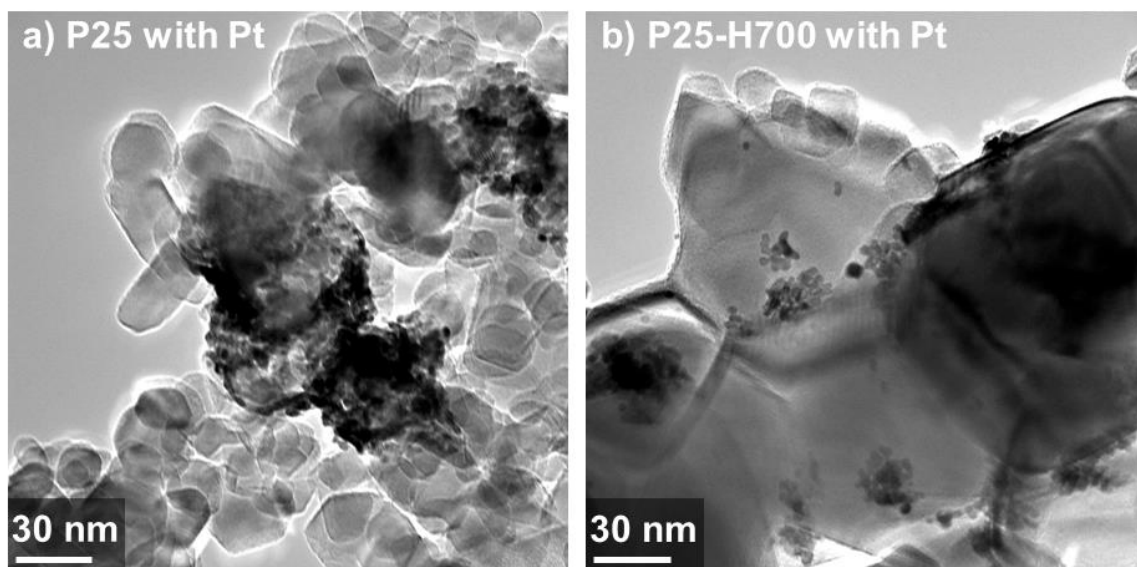


Figure S3. TEM images of (a) P25 and (b) P25-H700 with 2.0 wt.% Pt after photocatalytic H₂ evolution from 50 vol.% aqueous ethanol solutions under 380-nm irradiation.

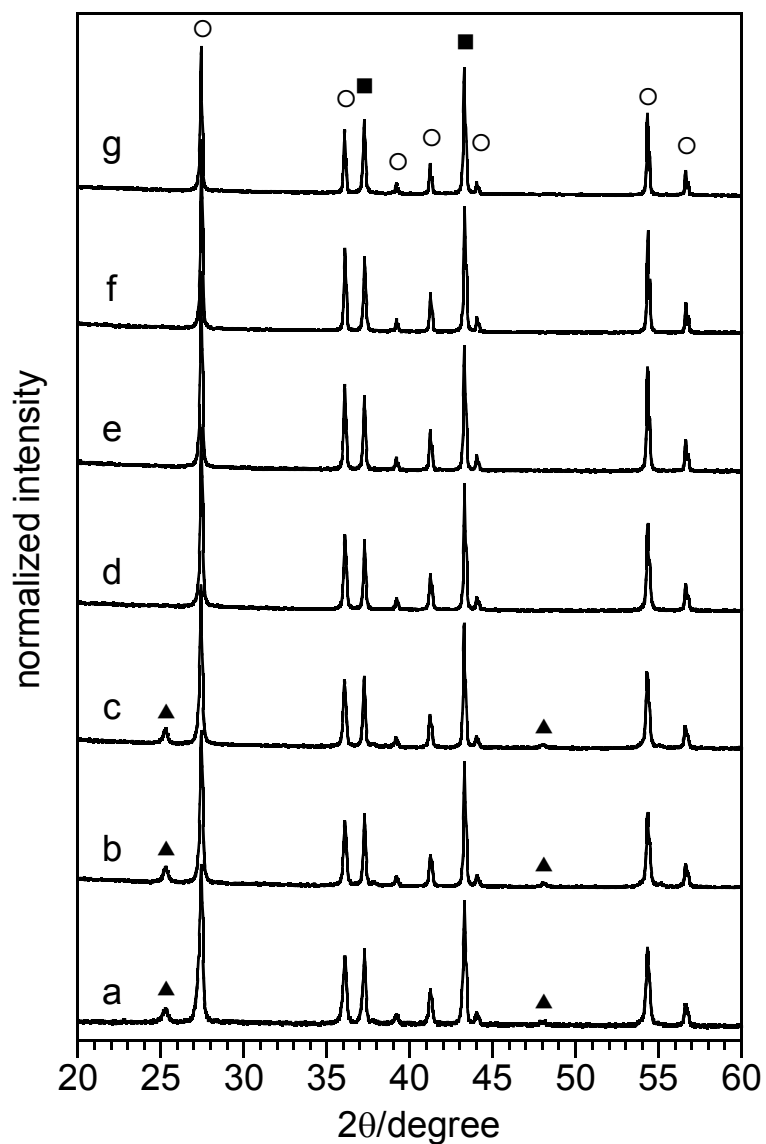


Figure S4. XRD patterns of H₂-reduced TiO₂ after calcination at (a) 300 °C, (b) 500 °C, (c) 700 °C, (d) 800 °C, (e) 900 °C, (f) 1000 °C, and (g) 1100 °C: (▲) anatase TiO₂, (○) rutile TiO₂, and (■) internal standard NiO. The TiO₂ was first calcined and then reduced with H₂ at 700 °C.

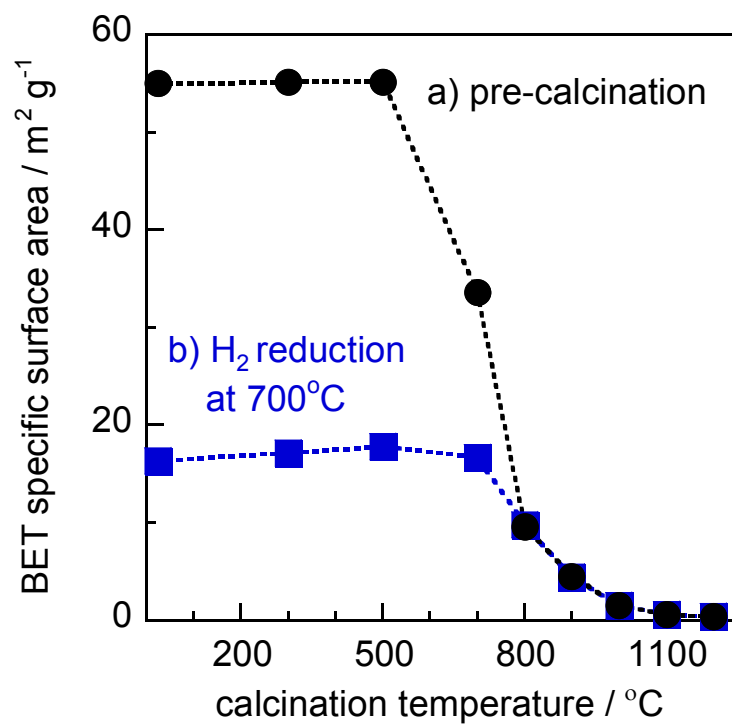


Figure S5. BET specific surface area of (a) TiO₂ P25 calcined at different temperatures, and (b) TiO₂ reduced with H₂ at 700°C after calcination.

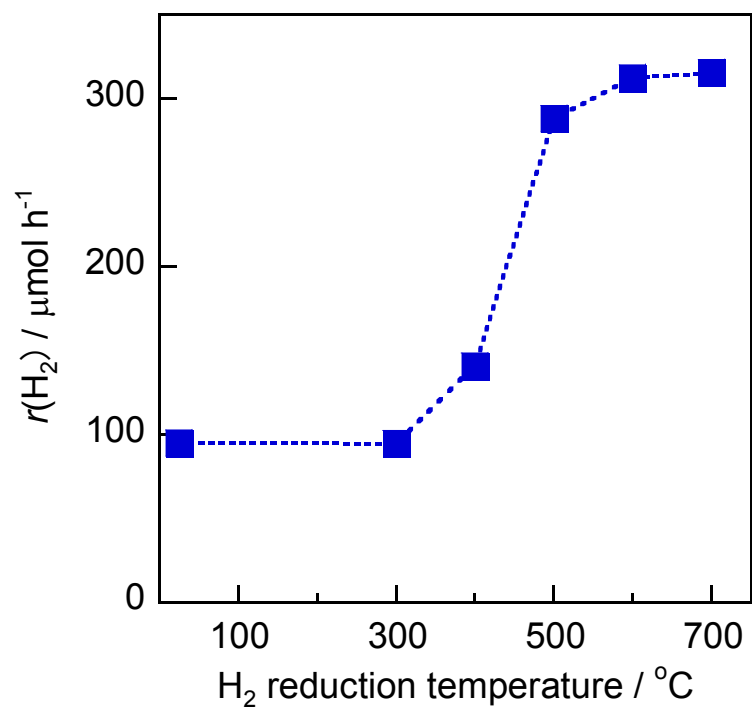


Figure S6. Effect of H₂ treatment temperature on the rate of photocatalytic H₂ evolution over phase-pure rutile P900 (Photocatalyst: 50 mg TiO₂. Solution: 50 vol.% aqueous ethanol solutions containing H₂PtCl₆ corresponding to 2.0 wt.% Pt, 9.0 mL. Light source: 380-nm LEDs). P900 denotes TiO₂ P25 calcined at 900°C.

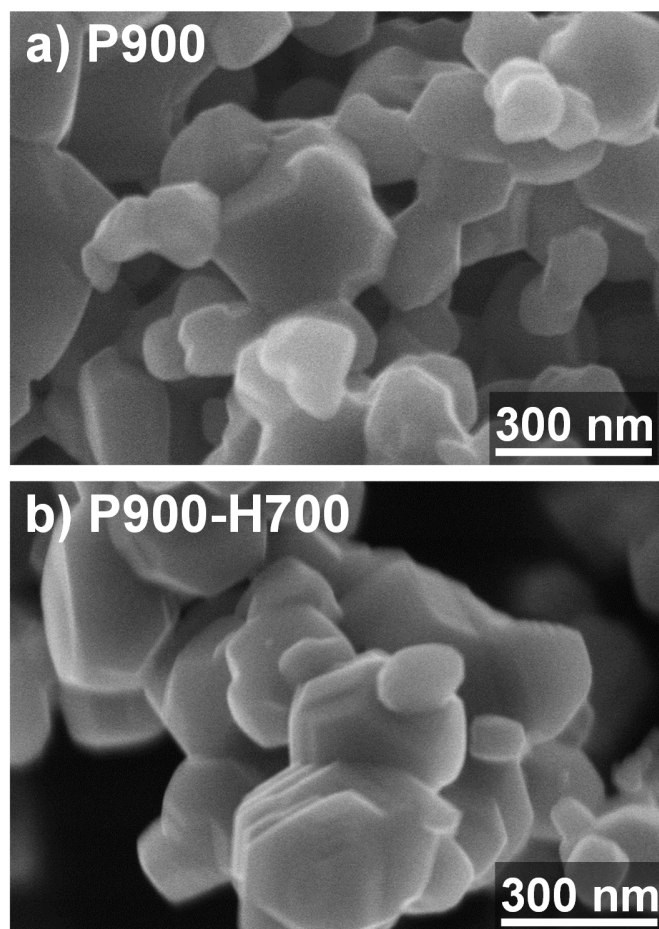


Figure S7. SEM images of (a) P900, and (b) P900 reduced with H_2 at 700°C , denoted as P900-H700. BET specific surface area was measured to be $4.5 \text{ m}^2 \text{ g}^{-1}$ for P900 and $4.4 \text{ m}^2 \text{ g}^{-1}$ for P900-H700. The average particle diameters were estimated to be about 320 nm from their BET specific surface areas using theoretical density of rutile TiO_2 (4.25 g cm^{-3}) assuming every particle is a sphere.

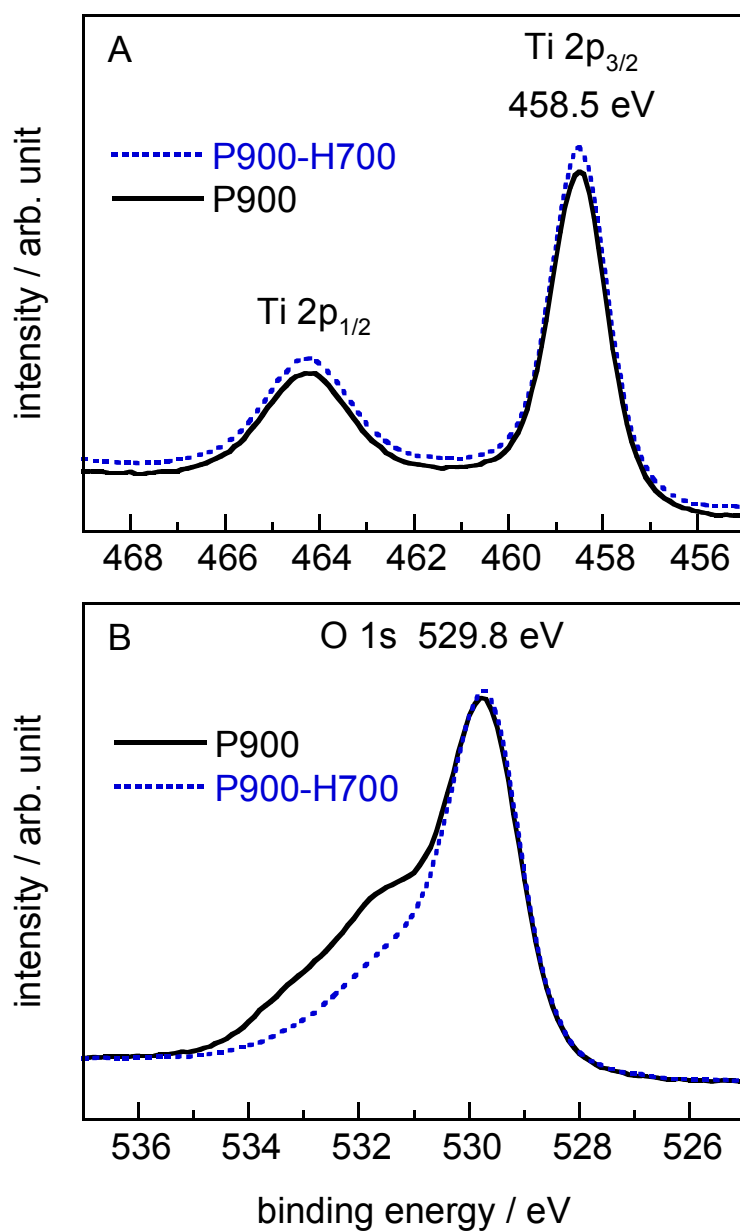


Figure S8. (A) Ti 2p X-ray photoelectron spectra (XPS) of P900 and P900-H700. The binding energy of 458.5 eV for Ti 2p_{3/2} is similar to the literature value for Ti⁴⁺ in TiO₂. This indicates that the amount of Ti³⁺ ions is small on the surface of H₂-reduced TiO₂. (B) O 1s XPS of P900 and P900-H700. The peak at 529.8 eV is assigned to lattice oxygen of TiO₂.

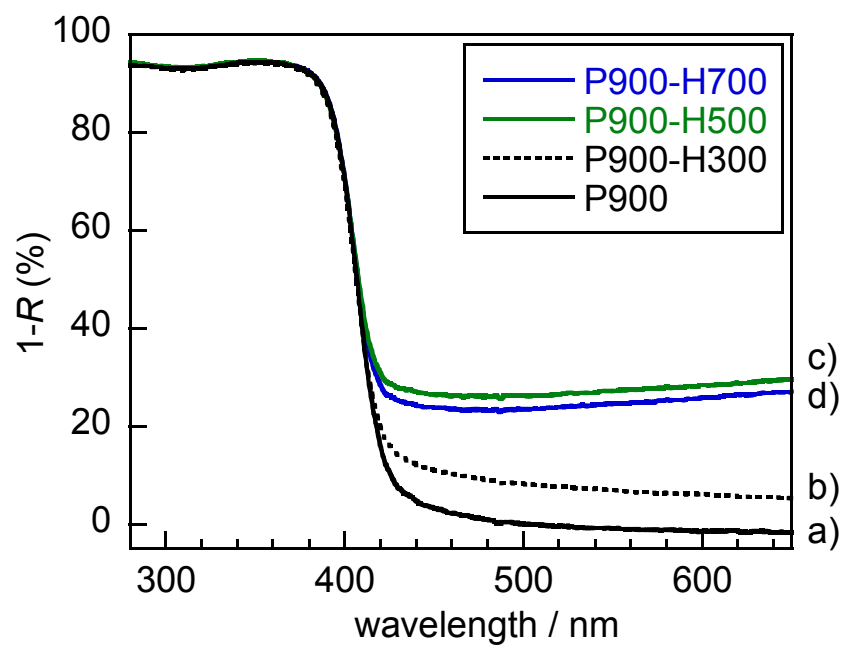


Figure S9. Diffuse reflectance UV-visible absorption spectra of (a) P900, (b) P900-H300, (c) P900-H500, and (d) P900-H700.

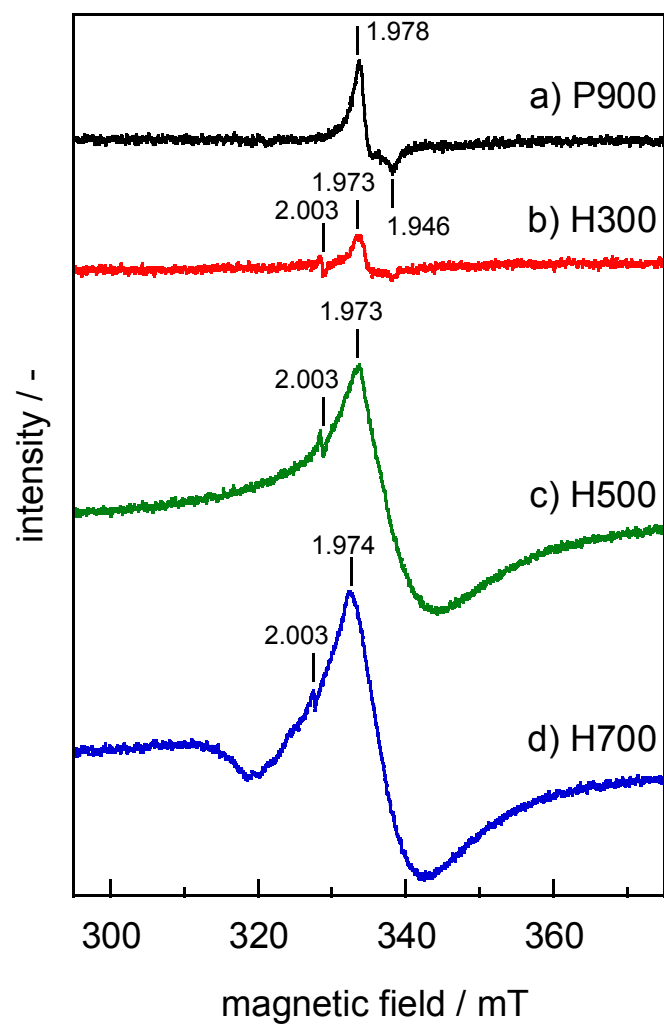


Figure S10. ESR spectra of TiO₂ particles monitored at -150 °C in the dark. (a) P900, (b) P900-H300, (c) P900-H500, and (d) P900-H700.